STRUCTURAL STUDY OF SOME LITHIUM BOROPHOSPHATE GLASSES USING DENSITY, HARDNESS AND INFRARED SPECTROSCOPY

A. M. Nassar, E.Nabhan, Al-Sh. Ramadan

Phys. Dept. Faculty of Science (Girls branch) Al Azhar university, Nasr city, Cairo, Egypt.

ABSTRACT

Glasses in the system [$50Li_2O-xB_2O_3-(50-x)P_2O_5$] ($10 \leq x \leq 27.5$), have been prepared by the melt quenching technique. Density, molar volume, hardness and Ft-IR spectroscopy have been employed to study the role of B_2O_3 on the structure of the glass network. The results of density and hardness showed that both increased as P_2O_5 is replaced by B_2O_5 [as y was increased from 0.2 up to 0.4 where ($y = B_2O_3/(B_2O_3+P_2O_5)$)]. After $Y \approx 0.4$ both of them decreased. Infrared spectra reveal that with the replacement P-O-B bonds are present at very low B_2O_3 content and their relative amount increased within the whole range of B_2O_3. BO_4 tetrahedral groups are predominant (~ 100%) up to 15 mole% B_2O_3. Then, the proportion of BO_3 units starts to appear.

1. INTRODUCTION

Alkali borate glasses with high ionic conductivity are receiving considerable attention because of their unique properties and their potential applications [1-4]. The role of alkali oxides in borate network is to modify the host structure by the transformation of BO_3 to BO_4 units. Previous studies [5-7] showed that the presence of B_2O_3 in the matrix of alkali phosphate improves the glass quality and enhance IR transmission. Also borophosphate glasses have a variety of other useful properties, where they can be used as fast ion conductors [8], zinc borophosphate can be used as glass solders [9], these glasses exhibit also high chemical durability.

The coordination of more than one former oxide such as P_2O_5 and B_2O_3, have interesting subject to study. The properties of such mixed former glasses are specific to the matrix being differ from the properties of either pure borate or pure phosphate networks. The basic units of pure borate glasses are BO_3, whereas the basic units of pure phosphate glasses are PO_4 tetrahedra. The addition of a modifier oxide to borate and phosphate networks has different effects. In a borate network, the addition of a modifier oxide increases the degree of polymenzation, the alkali oxide change the coordinates of boron from trigonal to tetrahedral, and the basic units changes from BO_3 to BO_4. In phosphate network, the addition of alkali oxide has the opposite effect, it has a deplymenzation effect, the extra oxygen atoms introduced by the alkali oxides form negative non-bridging oxygen (NBO) sites, whose charge is compensated by the positive charge of the alkali cation [10,11].

Borophosphate glasses possess a variety of useful properties. Alkali and silver borophosphate glasses are fast ion conductors [12,13]. Koudelka and Moser [14,15] have studied zinc borophosphate and zinc-lead borophosphate where they found that the addition of B_2O_3 increases T_g and they attributed it to the increased crosslinking and hence the dimensionality of the network. IR spectra revealed the presence of P-O-B linkages. It has also been observed that ionic conductivies in borophosphate are higher than that of corresponding binary borate and phosphate glasses.

In this article, we report a wide range of structural investigations for some lithium borophosphate glasses. Their physical properties such as density, molar volume, hardness will be measured. Infrared will be used. to investigate the structure and an available model will be applied.

2. EXPERIMENTAL

2.1) Sample preparation

An oxide glass system of the composition [$50Li_2O – xB_2O_3 - (50 - x) P_2O_5$] was prepared on the bases of the molecular percentage, within the glass formation limits $10 \leq x \leq 27.5$.

These samples were prepared in batches of 10 g. The compositions of the selected glasses were prepared by the conventional melt quenching method. The starting materials Li_2CO_3, $(NH_4)_2HPO_4$ and H_3BO_3 (all of analar grade) were mixed thoroughly by powdering in an agate mortar for half an hour to obtain well mixed fine powder. The ground mixture was heated in a platinum crucible at 450°C for about 1.5 h, then at 600'C for another 1.5h in order to decompose Li_2CO_3 and $NH_4)_2$ HPO_4. The batches were then melted at 1000°C for about one hour, meanwhile the batches were stirred several times to ensure complete homogeneity. The clear, bubble-free melted mixture was poured on a preheated copper plate at 200°C to avoid shattering of the quenched sample and pressed by another preheated copper plate. Thus, colorless, transparent [$50Li_2O$- xB_2O_3-$(50-x)$ P_2O_5] mole% glass was obtained.

Due to the different proposed measurements, the samples were divided into two parts. One part was powdered to suit Infrared and X-ray measurements. The second part was used in its solid form to suit the density and other measurements.

The prepared glass samples were investigated by means of (XRD) to confirm the amorphous nature of the samples. (XRD) measurements were performed. using a Philips Analytical X-ray diffraction system, type PW 3710 with the Cu – tube anode to check the non-crystalline nature of the glass samples.

The obtained XRD diffraction patterns are shown in Fig (1). This confirms that the prepared samples are completely amorphous. and the absence of any crystalline phase due to the absence of any sharp peaks in X-ray diffraction.
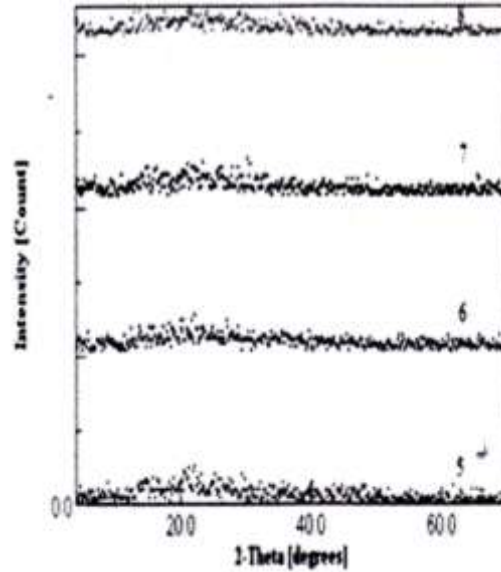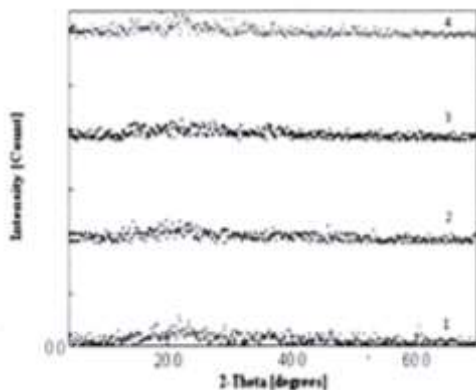
Fig (1) XRD patterns of all the studied glass samples.

2.2) Density and molar volume:

2-2-l) Density measurements:

The density of the prepared glasses was determined using Archimedes method. Each sample was weighed in air and after then immersed in toluene at room temperature. The density of the samples was calculated according to the following formula:

$$\rho_{ex} = \frac{(Wa)}{Wa - Wt} \rho_t \qquad (1)$$

Where ρ_{ex} is the experimental density of the glass sample, W_a. is the weight of the glass sample in air, W_t, is the weight of the glass sample in toluene, ρ_t is the density of toluene,($\rho_t = 0.865$ gm/cm^3 at RT) [16,l7].

The theoretical density of the samples was calculated from the following formula:

$$\rho_{theo} = 1/\sum_i (a_i/\rho_i) \qquad (2)$$

Where the nominator represents the mass of one gram of the sample and the denominator is represented by the summation of a_i over ρ_i, where a_i is the weight fraction of the oxides used in preparing the samples and pi is the density of these oxides forming the sample.

2-2-2) Molar volume calculations:

The following formula was applied for calculating the experimental molar volume

(V_m) of the investigated glass samples in the present work,

$$V_m = \frac{\sum wi}{\rho_{ex}} \qquad (3)$$

Where V_m is the molar volume of a glass sample, $\sum W_i$ represent the mean molecular weight of the glass sample, ρ_{ex} is the experimentally obtained density of such glass sample [18].

The theoretical molar volume (V_m) of the investigated glass samples is calculated from:

$$V_m = \frac{\sum wi}{\rho_{theo}} \qquad (4)$$

2-3) Micro hardness:

A Vicker's diamond indentor was used in a standard micro hardness tester (Leco AMH 100, USA) for specimen indentation.

High polishing was necessary for obtaining smooth, flat parallel surfaces before indentation testing. A load of 250 g applied for 15 s was used to make indentations in specimens of glass. Each sample was subjected to ten indentations at randomly selected areas, hence, erors in the measured values corespond to the standard deviation is about 2%. The diagonal length impressions were measured and the hardness number H was calculated according to a standard formula,

$$H_v = \frac{1.854F}{d^2} (Kg/mm^2) \qquad (5)$$

Where F is the indentation load (the force) and d is the diagonal length impression.

2-4) IR Spectroscopy and measurements:

Infrared spectroscopy is one of the most useful experimental techniques available for easy strucfural studies of glasses. It represents a powerful tool because it leads to structural aspects related to both the local units constituting the glass network and the anionic sites hosting the modifying metal cations [9,20].

Perken Elmer Spectrometer, model RTX, FTIR was used to obtain the IR spectra in the vibrational range from 4000 to 400cm^{-1}. The IR absorption spectra were recorded applying KBr disk method using Fourier Transform Infrared (FTIR) spectrometer at room temperature. The used apparatus gives directly the value of the vibrational energies of the present structure groups from the (FTIR) software.

3. **RESULTS AND DISCUSSION**

3.7 Density, molar volume and hardness

Density is an important and accurate property, which strongly reflects the fine changes in the glass structure; it is a measure of mass per unit volume. Fig (2), Fig(3), Fig(a) and Table (1) show the theoretical and experimental values of density (ρ), as well as the corresponding molar volume V_M and vicker microhardness of the studied glasses.

Table (1): theoretical and experimental density (ρ), molar volume V_M and. Hardness

| Composition%			Density (gm/cm^3)		Molar Volume(cm^3/mole)		Vicker's microhardness Kg/mm^2
50Li$_2$O-xB$_2$O$_3$-(50-x)P$_2$O$_5$			Exp.	Theo.	Exp.	Theo.	
50	- 10	- 40	2.479	2.128	31.739	36.975	374.67
50	-12.5	-37.5	2.549	2.114	30.158	36.364	378.33
50	-15	-35	2.522	2.100	29.746	35.745	380
50	-17.5	-32.5	2.555	2.087	28.672	35.102	448.67
50	-20	-30	2.579	2.073	27.704	34.466	352.33
50	-22.5	-27.5	2.508	2.059	27.773	33.809	403.33
50	- 25	-25	2.453	2.047	27.650	33.141	366
50	-27.5	-22.5	2.443	2.034	27.030	32.462	364.66
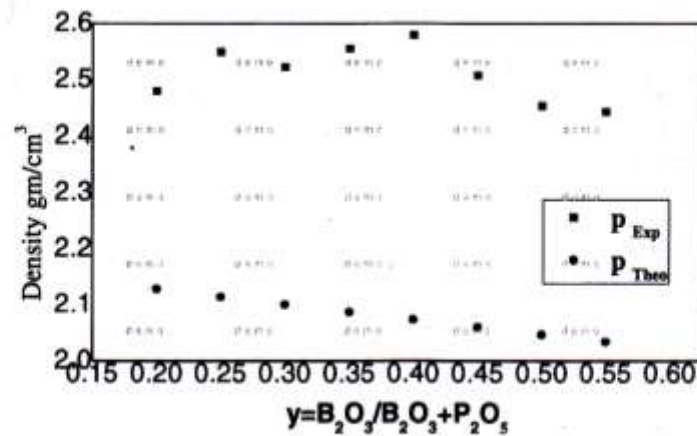
Fig (2) The variation of both the theoretical and Experimental density (ρ) as a function of y.
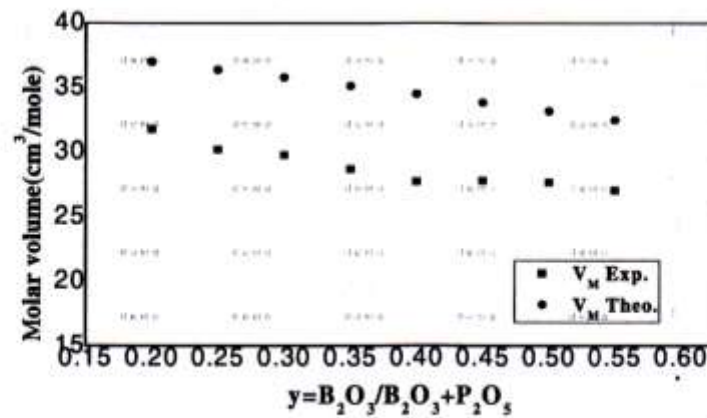

Fig (3) The variation of both the theoretical and experimental molar volume (V_M) as a function of y.
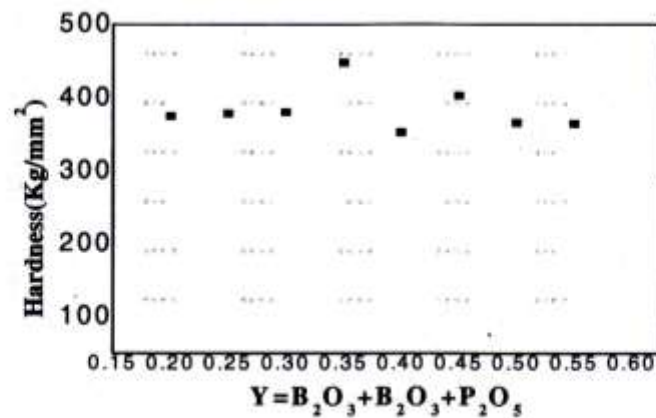

Fig (4) The variation of Hardness as a function of y.

Careful reading and analysis of the experimental density (ρ), and microhardness (H) given in Table (1) shows that:

1) The initial parts of B_2O_3 ($x \leq 20$) replacing P_2O_5 cause slight increase in both of the experimentally measured density (ρ) and microhardness (H).

2) Both of these materials characterizing parameters (p, H) are slightly decreased as the B_2O_3 parts exceed ($x \geq 20$).

3) The inflection point in (ρ, H) relations shown in figures (2) & (4) are nearly at (Y = 0.35), where [$y=B_2O_3/B_2O_3+P_2O_5$]. In other words, it is in agreement with a previous finding by Biakov a 123).

These changes in (p, H) may reflect some changes in the structure of the glass sample on increasing the B_2O_3 content, for example, the increase of both (ρ, H) may indicate that, the glass matrix overall becomes stronger and more rigid with increasing the B_2O_3 content due to the increase in cross-linking in between the phosphate chains in the glass network through B-O-P bonds.

The decrease in molar volume indicates a higher crosslinking of the glass network within the whole range of compositions.

3.2) Infrared

The infrared absorption spectra over the frequency range from (400 to 4000) for [50 Li_2O - X B_2O_3 - (50-X) P_2O_3] glass system, with $10 \leq x \leq 27.5$ mole% are represented in Fig (5) and the assignments of the detected absorption bands are sunrmarized in Table (2).

Careful comparison of such spectra and trials following different proportions, leads to the following assignments:

1- The band at - 1640 cm-' is assigned to the vibration of OH group.

2- The absorption band at around (1350-1450) cm^{-1} is a small peak attributes to the B-O stretching vibrations of trigonal BO_3 units and increases with the increase of boron oxide.

Table (2): Assignments of the observed bands of the alkali Borate, alkali phosphate and borophosphate glasses

| Band positions cm^{-1}	Suggested assignment	References
1640	Deformation vibration of free water	24,25
1200-1450	B-O is stretching vibrations of trigonal BO_3 units	26,27,28
850-1200	B-O is stretching vibrations of tetrahedral BO_4 units	26,27,24,29
600-800	Originating from bending vibrations of the borate network	26,27
1180 -1280	Symmetric and Asymmetric stretching vibration of P-O bonds in O-P-O groups $(PO_2)s$, asy	30,31,32,33
1200	Symmetric vibrations of two non-bridging oxygen atoms in PO_4 tetrahedra.	29,30
1100	Asymmetric vibrations of P-O	30,31,34,35
900	Asymmetric stretching vibration of $(P-O-P)_{As}$ in P-O-P linkages.	24,29,30,31
840	Symmetric stretching vibration of P-O-B	24,29,30,31
745-775	Symmetric stretching vibration of $(P-O-P)_s$ in P-O-P linkages	24,29,30,31
450-500	Deformation mode of PO_4	24,29,30,31
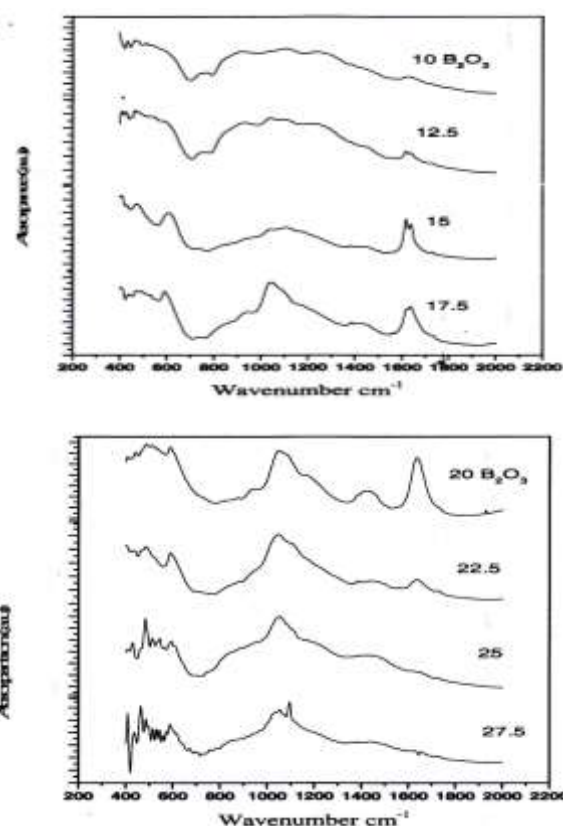
Fig. (5) Infrared absorption spectra of the glass system (50 Li_2O – X B_2O_3 – (50-X) P_2O_5) where $10 \leq x \leq 27.5$

3- The absorption band around (1180-1280) cm-' attributes to symmetric and asymmetric stretching vibrations of P-O bonds in O-P-O groups which is a broadband and becomes weaker as B_2O_3 content increased.

4- The absorption band at around (1200) cm^{-1} can be attributed to symmetric vibrations of two non-bridging oxygen atoms in PO_4 tetrahedra which is a broadband and becomes weaker as B_2O_3 content increased.

5- The absorption band at around (1200) cm^{-1} is attributed to the asymmetric vibrations of P-O$^-$ and it gets weaker as B_2O_3 content increased.

6- The absorption band at around (1000) cm^{-1} is attributed to P-O$^-$ symmetric stretching vibrations of PO_4 tetrahedra in the chain structure and becomes weaker as B_2O_3 content increased.

7- The relatively weaker absorption band at (950) cm^{-1} can be attributed to B-O stretching modes of BO_4 units which increases in intensity towards the increase of boron oxide.

8- The absorption band around (900) cm^{-1} can be attributed to $(P-O-P)_{As}$ asymmetric vibrations it gets weaker, shifted to higher wave number and its intensity decreased as B_2O_3 content increased.

9- The absorption band around (840) cm^{-1} can be attributed to (P-O-B) symmetric vibrations. It is a small peak and increases as boron oxide increased.

10- The absorption band around (750)cm^{-1} can be attributed to (P-O-P)s symmetric vibrations. It is a small peak and becomes weaker. as B_2O_3 content increased.

11- The absorption band around (600-800) cm-t can be attributed to the bending vibrations of B-O-B linkages. It is a small peak and increase in intensity as B_2O_3. content increases.

12- The absorption band around (450-500) cm^{-1} can be attributed to $(PO_4)^{3-}$. Such peak strong one and becomes weaker as B_2O_3 coiltert increased.

DISCUSSION:

In the binary glass $XM_2O-(1-X)$ P_2O_5, the ratio of BOAIBO within the whole range of $0 \leq$ x $\leq$ 0 .7 5can be predicted by the following equation (4):

$$BO/NBO = 0.5 (3-4x) \qquad (6)$$

Where (BO) are the bridging oxygens, (NBO) are the non- bridging oxygens and X is the alkali concentration. In the studied glass system the alkali concentration is constant (Li_2O concentration= 50 mole %). So, before adding B_2O_3:

$$BO/NBO = 0.5 [3-(4 \times 0.5)] = 0.5$$

In other words, bridging and non-bridging proportions are equal in the parent glass [36,37]

As P_2O_5 is replaced by the glass forming B_2O_3, new structural groups will appear as a result of the bridging between phosphate units and borate units [38].

The different types of phosphate species (Q_2 and Q_1 units) are bonded to either BO_3 or BO_4 boron groups. Therefore a transition from a phosphate to a borophosphate glass network occurs [22] where Q_2 & Q_1 represent The resulting depolymerisation of the phosphate network with the addition of alkali oxide, M_2O by the pseudo-reaction model [164], where the index n in Q, (where n - 0, 1,2,3) is the number of bridging oxygens per PO_4 tetrahedron [39].

$$2Q_n + M_2O \longrightarrow 2Q_{n-1} \qquad (7)$$
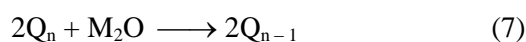
Due to the simultaneous presence of borate and phosphate groups in the sample, the spectral region (600-1200) reflects the overlapping of the characteristic bands of the expected BO_4, P-O-P$_{(S, AS)}$, and P-O-B groups.

So, IR deconvolution is made by an origin program in the region (600-1600) cm^{-1} to achieve the best fits for all the experimental spectra and to separate this overlapping and define the accurate position for each group by calculating the relative area for each position resulting from deconvolution assignment positions. (The position of each band, bandwidth and its intensity are adjustable parameters during the fitting) [40].

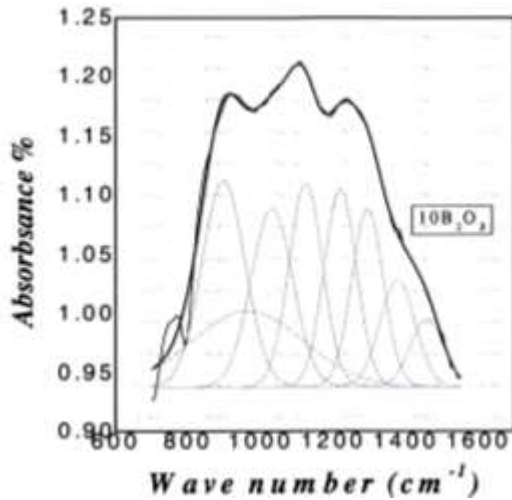An example of deconvoluted IR spectra is represented in Fig (5).

Fig (5) An example of the deconvolution of one of the studied glass sample

When P_2O_5 is replaced with B_2O_3, some new bands are observed around (600-800)cm^{-1} is assigned to bond bending vibration of B-O-B linkages which increase in intensity as B_2O_3 increased, at (950) cm^{-1} which is attributed to BO_4 increases as B_2O_3 content increases (BO_4) groups exists till the ratio of 20% mole of B_2O_3, it then decreases which may be due to the transformation from BO_4 tetrahedral to BO_4 triagonal and this is in agreement with B. K. Money et al. who concluded that at more than 20% B_2O_3, there is anomalous behavior BO_4 converts to BO_4. The phosphate units progressively disappear as B_2O_3 content increases (phosphate units bridge borate groups) [21].

By following the absorption bands results from deconvolution analysis, there is still an overlapping in the same region (600 to 1200), different structural groups cannot be distinguished.

Another useful way to separate and assign various bonds is by what is called a structure model. It is a model developed for borophosphate structure to allow one to check the plausibility of the various experimental findings, such as the relative fractions of non-bridging oxygens (NBOs), bridging oxygens (BOs) (i.e, P-O-P, B-O-B and P-O-B bonds) present in the borophosphate glass system $[0.45Li_2O – xB_2O_{3-}(0.55-x) P_2O_5]$ [41].

The relative fractions of the four possible oxygen species can be described by:

$$f_{NBO} = [N_{NBOP} - Y * (N_4*2 + N_3*1)] / N_O \qquad (8)$$

$$\hat{f}_{POB} = \varepsilon *2*Y*(1-Y)*(1-\hat{f}_{NBO}) \qquad (9)$$

$$f_{POP} = (1-f_{POB} *\varepsilon / 1- \hat{f}_{POB}) * (1-Y)^2 * (1-\hat{f}_{NBO}) \qquad (10)$$

$$\hat{f}_{BOB} = (1-f_{POB} *\varepsilon / 1- \hat{f}_{POB}) * Y^2 * (1-\hat{f}_{NBO}) \qquad (11)$$

$$\hat{f}_{NBO} + \hat{f}_{POB} + \hat{f}_{POP} + \hat{f}_{BOB} = 1 \qquad (12)$$

Where f_{NBO}, f_{POB}, f_{POP}, f_{BOB} are the relative fractions of NBOs, P-O-B, P-O-P and B-O-B bonds respectively. NNsop represents the number of NBOs in one formula unit of the parent phosphate glass and it can be calculated from equation (6), N_o is the total number of oxygens per formula unit, Y is the B_2O_3 molecular percentage, N_4, N_3 are the relative fractions of BO_4 and BO_3 units, respectively, and they can be calculated from relative area calculated for their positions from deconvolution results and ε is the preference factor for the P-O-B formation it is equal to 1.65.

^{11}B MAS NMR studies on $[0.50Li_2O - (0.50 - x) P_2O_5 – xB_2O_3]$ glasses indicated that BO_3 units are predominant ($N_4 = 100\%$) up to x - 0.15, then Na progressively decreases and the fraction of BO_3 units increases with the further B_2O_3 addition. ^{31}P MAS NMR spectra in this glassy system further showed that the increase of B_2O_3 content leads to the increase of Q_1 phosphate units as well as P-O–B linkages, and the decrease of Q_2 phosphate units. In addition, ^{7}Li MAS NMR confirmed that Li atoms remain a four-coordinated environment with B_2O_3 addition in the $[0.50Li_2O - (0.50 - x) P_2O_5 - xB_2O_3]$ glasses [22]. The fraction BO_4 units (N_4) and hence the fraction of BO_3 units (N_3, where $N_3 = 1-N_4$).

Due to the studied glass system $[0.50Li_2O- xB_2O_3 - (0.50 - x) P_2O_5]$ is similar to the previously studied glass system $[0.45Li_2O- xB_2O_3-(0.55-x) P_2O_5]$ with XPS technique so, the same preference factor is used with different way as the present glass system depends on the deconvolution results as mentioned above.
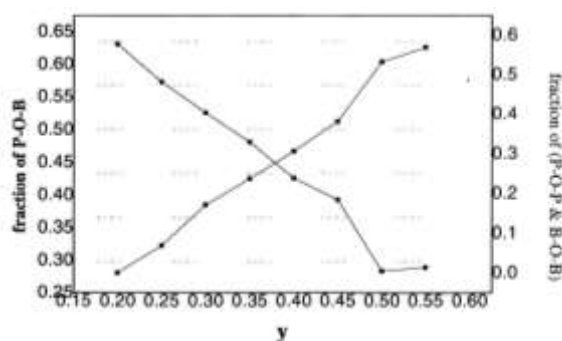
Fig (6) The fractional P-O-B and P-O-P& B-O-B bonds calculated from the structure model through deconvolution results as a function of relative content y.

From fig (6) the proportions of P-O-P & B-O-B decrease, and the concentration of P-O-B bonds increases with the rising B_2O_3 content [42].
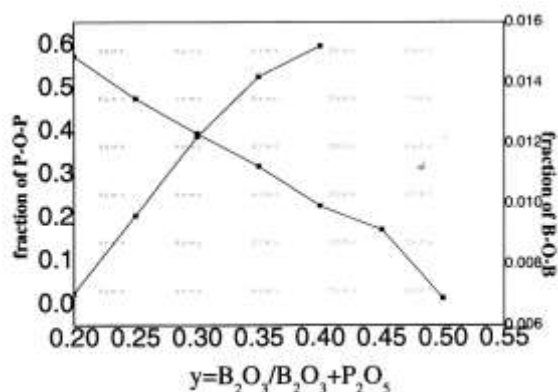

Fig (7) The fractional P-O-P and B-O-B bonds calculated from the structure model through deconvolution results as a function of relative content y.

From fig Q) the bridging of P_2O_5 decrease and the bridging of B_2O_3 increase.

CONCLUSION

The appearance of the new band P-O-B at nearly $840cm^{-1}$ is consistent with the presence of new borophosphate units and the phosphate units bridging the borate groups. The higher the boron content the higher the P-O-B bonds and Q_1 phosphate groups.

The same results are concluded through using NMR techniques. The NMR results show two important structural features as the BzOl content increases in the lithium borophosphate glasses [21,22].

1. P-O-B bonds are present at very low B_2O_3 content and their relative amount increases within the whole range of B_2O_3 as shown in fig (6).

2. BO_4 tetrahedral borate groups are predominant - l00%o up to 15 mole% B_2O_3, Then, proportion of BO_3 units increases as shown in fig (5).

And this in agreement with the results for density, molar volume and Hardness. As the density and hardness increase with the increase of borate content and this may be due to the existence of BO_4 group and formation of P-O-B bonds which increase the bridging between the borophosphate units. Then the introduction of BO: units after then when x excesses 20 mole% are responsible for the decrease in density and hardness. The molar volume decreases for all proportions of borate content.

REFERENCES

1. M. Balkanski, R.F.Wallis, J. Deppe, M. Massot, Mater.Sci.Eng.B .,12(1992)281.

2. J.Swenson and L. BOrjesson, Phys. Rev.B, 57(1998)1,3514.

3. M.Wollenhaupt, H. Ahrens, P.Frobel, K.Barner, E.Giessinger, R.Braunst, J.Non-Cryst. S ol ids, 27 8(2000) 191.

4. G Ramadevudu, M.Shareefuddin, N. Sunitha Bai, M. Lakshmipathi Rao, M. Narashimha, J.Non-Cryst. Solids, 27 8 (2000)205 .

5. S.K.Hong, D.SJung , J.S.S Cho, Y.C.Kang. J. Non-Cryst.Solids 354(2008)3012.

6. A. F. L. Almeida, D. Thomazim, I. F. Vasconcelos, M.A.Valente, A.S.B. Sombra, Int J. Inorg. Mater.3 (2001) 829.

7. A.F.L.Almeida, I.F. Vasconcelos, M. A. Valente, A.S.B. Sombra, Physica 8, 322 (2002) 276.

8. S.Kumar, P.Vinatier, A.Levasseur, K. J. Rao, J.Solid state Chem,I77(2004)1723.

9. R. K. Brow, D. R. Tallant, J.Non- Cryst. Solids 222 (1997) 396 .

10. A.Marotta, A.Buri, F.Branda, P.Pernics, A. Aronne, J.Non-Cryst.Solids,95&96(1987) 593.

11. Elbers, W.Strojek., L.Koudelka, H.Eckert, Solid State Nucl.Magn.Reson,ZT (2005) 6s.

12. K.J.Rao "Structural Chemistry of Glasses", Elsevier, Amsterdam, (2002).

13. M.Scagliotti, M.Villa, G.Chiodelli, J.Non-Cryst.Solids, 93(1987)350.

14. L. Koudelka, P.Mosner, Mater.Lett,42 (2000) 194.

15. L.Koudelka, P.Mosner J.Non-Cryst.Solids, 293-295 (2001) 635.

16. N.J. Kim, Y. H. La, S. H. Im, W.-T. Han, and B. K. Ryu, Electron. Mater. Lett., 5 (2009) 4.

17. N. Sugimito, J. Am. Ceram. Soc., 85 (2002) 1083.

18. M. D. Thombare," International Journal of Research in pure applied physics",4(2) (2014) 9 .

19. A. Witkowska, J. Regbicki and A.D. Eicco, J. Alloys Compd,324(2003)109.

20. E. I. Kamitsos, J. Phys . Chem. Glasses,44 (2003)79.

21. B. K. Money, K. Hariharan, Solids State Ionics, ll9, (2008) 1273.

22. F. Munoz, L. Montagne, L. Pascual, A. Duran, J. Non-Cryst. Solids, 355 (2009) 2571.

23. L.G. Baikova, Yu. K. Fedorov, V.P. Pukh, L.V. Tikhonova, T.P. Kazarutikova, A.B. Sinani, and S.I. Nikitina, Glass Physics and Chemistery,29, No(3) (2003) 276.

24. A.Chahine, M.Et-Tabirou, M.El benaissi, M.Haddad, and J.L.Pascal. Mater. Chem. Phys., 84, (2004) 341 .

25. B.Bridge, and N.D.Patel. J.Non-Cryst. Solids, 27 (1973) 91.

26. E.I. Kamitsos, M.A. Karakassides and G.D. Chryssikos, Phys. Chem. Glasses, 28 (1987) 203.

27. Y.H. Yun and P.J. Bray, J. Non-f&t. Solids, 44 (1981) 227 .

28. E.I. Kamitsos, G.D. Chryssikos, J. Mol. Struct, (1991) 247.

29. S. Kumar, P. Vinatier, A. Levasseur, K. J. Rao, J. Solid State Chem, 177 (2004) 1723.

30. S.W. Martin, Eur. J. Solid State Inorg. Chem., 1 (1991) 163.

31. S. Agathopoulos, D. U. Tulyaganov, J. M. G. Ventura, S. Kannan, A. Saranti, M. A. Karakassides, and J. M. F. Ferri- era, J. Non-Cryst. Solids, 352 (2006) 322.

32. R. K. Brow, D. R. Tallant, S. T. Myers, C. C. Phifer, J. Non-Cryst, Solids, l91 (1995) 45.

33. G. B. Pakhomov, S. L. Neverov, Solid State Ionics, 119 (1999) 235.

34. P. Y. Shih, Mater. Chem. Phys. 84, (2004) 151.

35. R. F. Bartholomew, J. Non-Cryst. Solids T, (1972).22.

36. U. W. Wiench,M.Pruski,B. Tischendorf, J.U. Otaigbe, B.C. Sales, J. Non-Cryst. Solids, 263 (2000) 101.

37. S. W. Martin, C. A. Angell, J. Non-Cryst. Solids,83 (1986) 185.

38. P.S. Anantha, K. Hariharan, Materials Chemistry and Physics 89, (2005) 428.

39. J. R. Van Wazer, Phosphorus and its Compounds, Volume 1, Interscience, New York, 1958.

40. B. N. Nelson, G. J. Exarhos, J. Chem. Phys.71 (1979) 2739.

41. TH. DUCTHOa, R. Prasada Raoa, S. Admas. The Electrochemical Society ECS Trabsactions, 28(30) (2010) 187.

42. R. K. Brow, J. Non-Cyst. Solids, 194 (1996), 26.